NOISE BEHAVIOR IN GRIDDING RECONSTRUCTION

Carlos Mosquera, Pablo Irarrázabal, Dwight G. Nishimura*

Magnetic Resonance Systems Research Lab
Stanford University, Stanford, CA 94305, USA.

ABSTRACT

This paper addresses the properties of the noise in Gridding reconstruction, an algorithm for reconstruction from nonuniform samples . Sequences with time-varying gradients, such as Spiral or Projection Reconstruction (PR) techniques, are being increasingly used in Magnetic Resonance Imaging (MRI). Since these techniques sample k-space nonuniformly, some kind of algorithm is needed to map the data onto a Cartesian frame to allow an inverse Fourier transform through an FFT. We present here an analytical characterization of the image noise after Gridding and inverse Fourier transform for the most popular sampling techniques used in MRI.

1. INTRODUCTION

In many fields ranging from radio astronomy to Magnetic Resonance Imaging (MRI), Fourier inversion of data not falling on a Cartesian grid has been necessary. It is well known the considerable numerical advantage of the Discrete Fourier Transform through the use of the FFT, but in many occasions the samples are not on a Cartesian grid, so some kind of interpolation is necessary to obtain the values on a Cartesian grid. Many algorithms have been developed for reconstruction from nonuniform samples such as nearest-neighbor, truncated sinc function FIR interpolators and bilinear interpolation [1]. The technique known as Gridding reconstruction has proven to be very efficient in terms of computation and artifact levels [1]; in its earliest forms, different methods were used, such as cell summing, cell averaging and Gaussian methods, all of them compared in [2]. That algorithm has been deeply studied [1][3], but there is no clear understanding yet on the properties of the colored noise in the final data, goal of this work.

Gridding algorithm is not an interpolation technique in a strict sense, since it does not necessarily assign the same original value to sample points that fall on the Cartesian grid. O'Sullivan [1] shows that the optimal gridding method is convolution with a sinc function of infinite extent, followed by sampling onto a Cartesian grid, but practical considerations require that the infinite sinc function be replaced with a finite convolving function. The goal is to make the inverse transform of the new data as close as possible to the inverse transform of the original sampled data within some region of the image domain. The discrete implementation of the algorithm is as follows [4]:

$$M_{pq} = \frac{1}{\phi_{pq}} \sum_{\alpha} \sum_{\beta} \frac{M_{\alpha\beta}}{\rho_{\alpha\beta}} C(\|k_p, k_\alpha\|, \|k_q, k_\beta\|) \quad (1)$$

$$m_{ij} = \frac{1}{c_{ij} n^4} \sum_{p} \sum_{q} M_{pq} e^{i(\theta_{ip} + \theta_{jq})} \quad (2)$$

with $\theta_{ip} = \frac{2\pi}{n} i k_p$. M represents the noise in the Fourier domain, and m the noise in the object domain. Greek indexes are used for the original grid and Roman indexes for the uniform grid. The variable k is used for the discrete frequencies. C is the kernel used in gridding, and $\|a, b\|$ a distance that should be circular to prevent border effects, although in real situations a simple non circular distance is used, as will be the case here. The nonuniform sampling will introduce a nonuniform weighting, and a division by $\rho_{\alpha\beta}$, the estimated density of the sampling (predensity), is introduced, to compensate this effect. Since that estimate of the density is usually not exact, an additional correction is incorporated, the postdensity ϕ_{pq}. In the object domain a division by c_{ij}, the inverse 2DFT of the discrete kernel in the Fourier domain, is necessary to undo the effect of the convolution in the Fourier domain.

2. NOISE PROPERTIES

We computed the first and second statistics of the noise in the object domain, under the reasonable assumption of white noise for the MRI signal.

The **Input Noise** has zero mean $E(M_{\alpha\beta}) = 0$, and is uncorrelated. We will assume the same variance for both real and imaginary parts σ^2, with both parts uncorrelated.

Since the mean of the input noise is zero, the **Object Noise** also has zero mean:

$$E(M_{pq}) = \frac{1}{\phi_{pq}} \sum_{\alpha} \sum_{\beta} \frac{E(M_{\alpha\beta})}{\rho_{\alpha\beta}} C(\|k_p, k_\alpha\|, \|k_q, k_\beta\|) = 0 \quad (3)$$

$$E(m_{ij}) = \frac{1}{c_{ij} n^4} \sum_{p} \sum_{q} E(M_{pq}) e^{i(\theta_{ip} + \theta_{jq})} = 0 \quad (4)$$

After the whole reconstruction process, the object noise is going to be colored, so we need to compute the correlation in the final image. Using Equation 2 :

* Currently with D.T.C., ETSI Telecomunicación, Universidad de Vigo, Lagoas-Marcosende, Vigo 36200, SPAIN. E-mail: mosquera@dtc.uvigo.es

0-7803-2431-5/95 $4.00

$$E(m_{ij}m^*_{ln}) = \frac{1}{c_{ij}c_{ln}n^8} \cdot \sum_{p,q}\sum_{r,s} E(M_{pq}M^*_{rs})e^{i(\theta_{ip}+\theta_{jq}-\theta_{lr}-\theta_{ns})} \quad (5)$$

From there, and after some simple algebraic steps we can conclude that:

$$E(m_{ij}m^*_{ln}) = \frac{\sigma^2}{c_{ij}c_{ln}n^4}\mathrm{DFT}^{-1}_{4D}\left\{\frac{\Delta(p,q,-r,-s)}{\phi_{pq}\phi_{-r-s}}\right\} \quad (6)$$

where a new function has been defined

$$\Delta(p,q,r,s) = \sum_{\alpha,\beta}\frac{1}{\rho^2_{\alpha\beta}}C(\|k_p,k_\alpha\|,\|k_q,k_\beta\|) \cdot C(\|k_r,k_\alpha\|,\|k_s,k_\beta\|) \quad (7)$$

3. INTERPRETATION

Since the discussion is easier in two than in four dimensions, we will make some additional comments on the 1D case, extending that interpretation to 2D afterwards.

It can be proved that the 1D results are analogous to the 2D results:

$$E(m_i m^*_j) = \frac{\sigma^2}{c_i c_j n^2}\mathrm{DFT}^{-1}_{2D}\left\{\frac{\Delta(p,-q)}{\phi_p\phi_{-q}}\right\} \quad (8)$$

The expression

$$\Delta(p,q) = \sum_{\alpha}\frac{1}{\rho^2_\alpha}C(\|k_p,k_\alpha\|)C(\|k_q,k_\alpha\|) \quad (9)$$

gives the 'interpolated' value from the sampled data $\frac{1}{\rho_\alpha}C(\|k_q,k_\alpha\|)$, a kernel centered at q and weighted by the inverse of ρ_α, at the point p.

From that interpretation we can easily see that in the case of an original uniform grid the expression $\Delta(p,q)$ can be written as $\Delta(p-q)$ if a circular distance is used in the borders, because in that case points with the same separation will give the same value of $\Delta(p,q)$ (both densities, pre and post, are constant throughout the entire grid). Therefore, to get white noise in the object domain, we need a uniform grid with circular distance used in the gridding, since the Fourier transform of a Toeplitz matrix ($\Delta(p-q)$) is a diagonal matrix. And even in the uniform case the variance of the noise in the object domain will be nonuniform, unless the original grid is exactly upon the desired grid.

From a filter perspective the Gridding algorithm for the uniform case (DFT sampling) is a convolution, since the pre and post densities are constant, and the filter is spatially invariant. If the convolution is circular it can be thought as a product in the object domain after the IDFT, unitary transformation that preserves the noise as white, so the final result is white. But if the convolution is not circular, as is usually the case, we can represent the situation as in Figure 1 (again in one dimension) for the uniform sampling case. 2n samples are taken to consider the effect of noise samples outside the n samples region, so that the convolution can still be thought of as a circular convolution; this only works if the kernel width is less than n, usual case. A product is needed afterwards to keep only the central samples used in the IDFT. A decimator in the final stage will reduce the number of samples to n, the number we want. The variance changes through the object and the noise is no longer white, as can be noticed in the equivalent representation. In the first product, c_i' is the inverse transform of the kernel samples used, which does not necessarily coincide with c_i, unless the final grid lies exactly on the original one. The filter present before the final division keeps only the low frequencies. And then $\frac{1}{c_i}$ will cause high variance for values of c low. There is a simple explanation for this: if we do not perform circular convolution in the Fourier domain we are making some errors at the edges, that means, in the high frequencies. That error will spread over the whole object in the object domain, and will be amplified by low values of the kernel when dividing by the kernel in the object domain. But this is true not only for the noise. Even in a noiseless case, there will be reconstruction errors due to the division by c_i, that does not undo exactly the effect of the kernel in the Fourier domain, especially noticeable at those points where c_i is low.

The extension of those ideas to the 2D case is straightforward: $\Delta(p,q,r,s)$ gives the "interpolated" value from the sampled data $\frac{1}{\rho_{\alpha\beta}}C(\|k_r,k_\alpha\|,\|k_s,k_\beta\|)$, a kernel centered at the point (r,s) and weighted by the inverse of $\rho_{\alpha\beta}$, at the point (p,q). According to that interpretation, no important differences should be expected in the noise correlation between different techniques with similar density distributions, as long as sampling is fine enough, since 'interpolated' values from the weighted kernel will be similar. And the object noise will only be white for the case of a uniform grid and circular distance. Therefore, the noise is colored in any practical application, where neither the distance is circular nor the grid is uniform. Our task now is to see what that correlation between pixels is like for typical cases.

4. RESULTS AND DISCUSSION

We studied the behavior of the noise for different sampling schemes commonly used in MRI: 2DFT, Projection Reconstruction (PR) and Spiral trajectories. Although it is not necessary to make use of gridding for the 2DFT case (uniform sampling of k-space), it is worth doing it to see the effects on the noise and keep it as a reference. In the PR case, 60 radial lines were used; this technique provides higher sampling density near the origin. And 20 interleaved spirals form the Spiral trajectories, sampled in such a way that the linear velocity spiral is constant (ignoring the singularity at the origin). Sampling density is fairly constant in this case, one of the advantages of this technique versus PR.

In our computations the uniform grid obtained after applying gridding was 16x16 pixels, and a non circular distance was used. For the representation of the correlation we used the correlation coefficient:

$$\nu(ij,kl) = \frac{E(m_{ij}m^*_{kl})}{\sqrt{E\mid m_{ij}\mid^2 E\mid m_{kl}\mid^2}} \quad (10)$$

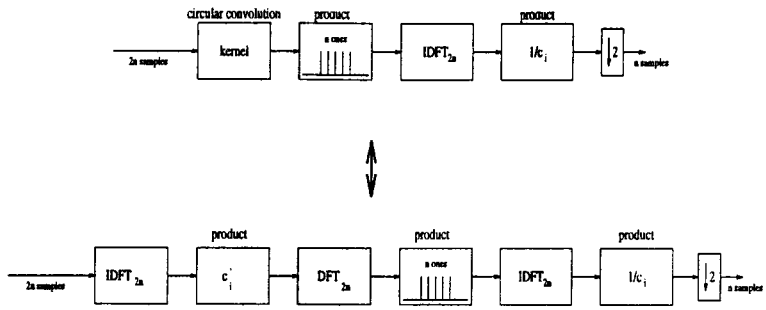

Figure 1: Non circular implementation of Gridding algorithm for the DFT case.

We will refer to it as just correlation for simplicity. Since we have four variables (the coordinates of two points), we decided to focus our attention on the correlation between the central pixel and the rest of the image (Figure 2), as well as the correlation between one corner and the other pixels (Figure 3): both are the extreme cases in our study. For the first case, the axes (x and y) have higher values of correlation, and that is why we decided to plot together the absolute value of the correlation for different cases on one of those axes. With the corner pixel, the correlation is higher along the sides of the image.

The choice of the convolution kernel has been object of extensive analysis [1][3]. We made the simulations with circularly symmetric triangular, Gaussian and Kaiser-Bessel kernels. Since the trend shown by the different kernels was essentially the same, we will only show here the results obtained with the triangular kernel; the conclusions are also valid for the other two kernels: the important factor is the extension of the kernel energy. So our results were obtained for different sizes of the kernel.

Figure 4 shows sections of the correlation between the central pixel and the rest of the image, for the three sampling grids ands for different sizes of the kernel. The 2DFT case is used as a reference for the other cases: had the convolution been circular the noise would be white, but as Figure 4 shows, border effects correlate pixels, correlation that becomes worse when the kernel gets wider. It can be noticed that there are no major differences between the different sampling techniques. And the correlation magnitude decays fairly fast, important to prevent possible artifacts in case of high noise. The same can be shown for the correlation between one corner and the rest of the image, with the same dependence on the size of the kernel, although now the corner is more correlated with the image than the center. In this latter case, PR sampling shows slightly higher values of correlation, whereas 2DFT and Spiral trajectories are very similar.

An apodization function can be used in some situations to soften the ringing effect caused by truncation of high frequencies. We also studied that case, and as apodization function we used the circularly symmetric Hamming window. Figure 5 illustrates the correlation with the central pixel in one case (Spiral trajectories) where apodization was used. Correlation functions are similar to the one shown for the different techniques, although the resemblance is larger between 2DFT and Spiral trajectories, as expected from the quasi-uniform sampling density of the Spiral trajectories. Because of the apodization, border effects lose importance now; but the correlation shape with the central pixel is broader than before, with less dependence on the size of the kernel in the 2DFT case. The Spiral trajectories correlation gets closer to the 2DFT correlation for large kernels, because of the rough density estimation with short kernels.

The variance of the noise in the object domain is another important element to consider. As explained before, non circularity is a key feature in this analysis, and even in the uniform case without apodization function border errors will cause a high variance of the noise at those points with the lowest values of the kernel c_{ij}, because of the division in the last stage of the algorithm. Of course, as soon as sampling leaves uniformity, the variance will no longer be uniform, with high values at those locations where c_{ij} is very low.

5. CONCLUSIONS

A method to compute the correlation of the object noise after Gridding reconstruction has been presented. With our main focus on MRI, the three most popular techniques used in MRI (2DFT, PR and Spiral trajectories) were analyzed. The three techniques yield similar results, something remarkable for practical applications, although the resemblance is especially high between the 2DFT sampling and Spiral trajectories, because of the properties of the latter sampling (close to uniform). If apodization is used, the different correlation shapes look alike as well, although the correlation with the central pixel is higher in general.

Gridding creates high values of noise variance at certain points in the object domain, because of the division by the kernel in the final stage. The same can be claimed about reconstruction errors of the image, even in the noiseless case, when a noncircular distance is used.

6. REFERENCES

[1] J. D. Sullivan, " A Fast Sinc Function Gridding Algorithm for Fourier Inversion in Computer Tomography," IEEE Trans. Medical Imaging, vol. MI-4, pp. 200-207, 1985.

[2] A. R. Thompson, R. N. Bracewell, "Interpolation and Fourier transformation of fringe visibilities," The Astronomical Journal, vol. 79, no. 1, pp. 11-24, 1974.

[3] J. I. Jackson, C. H. Meyer, D. G. Nishimura, A. Macovski, "Selection of a Convolution Function for Fourier Inversion Using Gridding," IEEE Trans. Medical Imaging, vol. MI-4, pp. 473-478, 1991.

[4] P. Irarrázabal, B. S. Hu, J. M. Pauly, D. G. Nishimura, "Spatially Resolved and Localized Real-Time Velocity Distribution," Magnetic Resonance in Medicine, vol. MRM 30, pp. 207-212, 1993.

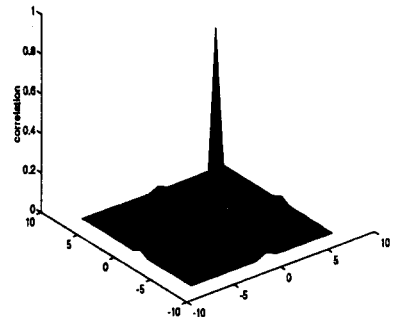

Figure 2: Correlation coefficient absolute value between the central pixel and the rest of the image (PR sampling).

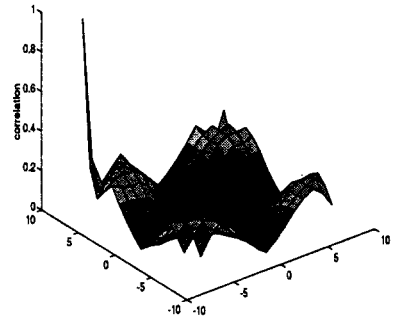

Figure 3: Correlation coefficient absolute value between one corner and the rest of the image (PR sampling).

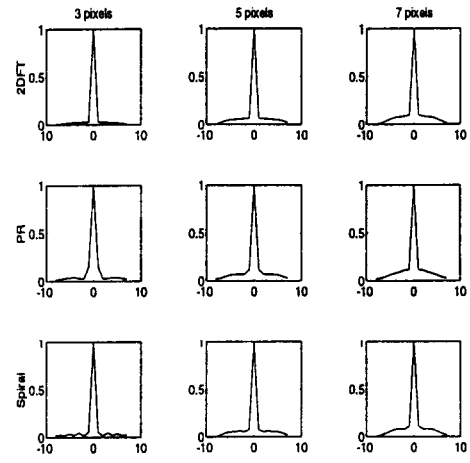

Figure 4: Correlation coefficient absolute value between the central pixel and one line of the image.

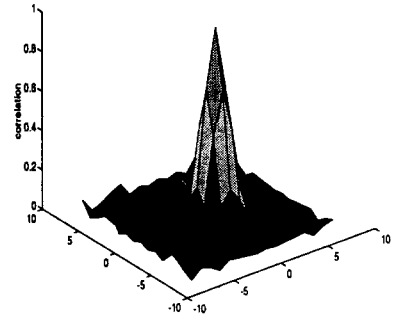

Figure 5: Correlation coefficient absolute value between the central pixel and the image, with apodization function used.